J. Chem. Sci. Vol. 126, No. 1, January 2014, pp. 55–63.

Effects of acid concentration on intramolecular charge transfer reaction of 4-(azetidinyl) benzonitrile in solution

BISWAJIT GUCHHAIT, TUHIN PRADHAN and RANJIT BISWAS*

Department of Chemical, Biological and Macromolecular Sciences, SN Bose National Centre for Basic Sciences, Block-JD, Sector-III, Salt Lake, Kolkata 700 098, India
e-mail: ranjit@bose.res.in

MS received 1 July 2013; revised 16 October 2013; accepted 18 October 2013

Abstract. Effects of acid concentration on excited state intramolecular charge transfer reaction of 4-(azetidinyl) benzonitrile (P4C) in aprotic (acetonitrile and ethyl acetate) and protic (ethanol) solvents have been studied by means of steady state absorption and fluorescence, and time resolved fluorescence spectroscopic techniques. While absorption and fluorescence bands of P4C have been found to be shifted towards higher energy with increasing acid concentration in acetonitrile and ethyl acetate, no significant dependence has been observed in ethanolic solutions. Reaction rate becomes increasingly slower with acid concentration in acetonitrile and ethyl acetate. In contrast, acid in ethanolic solutions does not produce such an effect on reaction rate. Time-dependent density functional theory calculations have been performed to understand the observed spectroscopic results.

Keywords. Intramolecular charge transfer; absorption and fluorescence; time resolved fluorescence measurements; acid concentration dependence; time-dependent density functional theory.

1. Introduction

Photoinduced intramolecular charge transfer (ICT) is a research area of fundamental interest as light induced charge separation plays an important role in photosynthesis and vision.[1–3] Experimental and theoretical studies of photo-induced ICT processes in basic science research[4–6] have increased significantly due to its biological importance. Of late, heterogeneous solution structures of various environments have been successfully probed by photoinduced ICT as its fluorescence characteristics strongly depend upon local polarity.[7] Fluorescence property of ICT molecule is used in characterizing various host systems which include biomolecular systems, pH and chemical sensors, molecular electronic devices, and bulk and confined liquids.[8–15] It has also been observed that photophysical properties of donor-pi-acceptor systems can be tuned by changing molecular structure and conjugation.[8] These applications encourage chemists and physicists to design and study photophysical behaviour of ICT molecules in various environments.

Fluorescence behaviours of 4-dimethylaminobenzonitrile (DMABN) and its derivatives have been extensively studied since the first discovery of dual emission due to excited state reaction.[8] Dual emission properties of 4-(azetidinyl) benzonitrile (P4C) in various environments have been previously studied using steady state and time resolved fluorescence techniques.[16–19] In polar solvents, P4C exhibits dual fluorescence where the long wavelength band appears due to intramolecular charge transfer. In this molecule, amine and cyano moieties act as donor and acceptor, respectively. The charge transfer state formation is sometime believed to involve an intramolecular twisting process in singlet excited state,[16(a)] although other mechanisms[16(b)] are also invoked. The photo-excitation of P4C to the locally excited (LE) state and thereby formation of charge transferred (CT) state are shown in scheme 1, where k_f and k_r are the forward and backward rate constants, respectively. k_{LE} and k_{CT} denote, respectively, the net (radiative *plus* non-radiative) rate constants for LE and CT states. CT state is more polar and thus stabilized by enhanced solute-solvent (dipole-dipole) interaction in polar media.[16] Interconversion between the LE and CT states is known as charge transfer step, which is much faster than the LE or CT population decay rates (or inversely, lifetimes) in polar solvents.[16]

Photophysical properties of various ICT molecules have been performed previously in different environments. Interestingly, heterogeneous nature and solution structural transition of water–alcohol binary mixtures have been probed by using the photo-response

*For correspondence

of P4C molecule.[7] Temperature-assisted aggregation of alcohol has also been observed by following the fluorescence response of the same solute.[20] Electrolyte-induced modulation of intramolecular charge transfer rate of P4C molecule in pure solvent has been explored and a non-monotonic dependence observed.[18]

To gain insight into the ICT of P4C in acidic media, we have performed detailed study of the acid concentration dependence of reaction equilibrium and rate constants for P4C in acetonitrile, ethyl acetate, and ethanol using steady state and time resolved fluorescence spectroscopic techniques. Note that although acid concentration and/or the pH-dependent photophysical behaviours of chemical and biological systems have been an area of intense research,[21–28] such a study for these model systems has not been done before. A fluorescence study reports that emission of dendrimer can be modulated by changing the pH.[21] Medium pH has also been shown to substantially affect the dual emission behaviour and excited state proton transfer of green fluorescent protein, and folding of proteins.[22] Again, binding of a dye with macromolecules has been shown to be dependent on medium pH.[23] In an earlier study, dopamine and some of its derivatives show pH-dependent oxidation and reduction potentials, which made it an important system to understand various biophysical processes.[24] It is known that charge transfer processes in supramolecular protein and DNA assemblies are central to the function of many biological processes. Pi-stacked bases in DNA facilitate electron transport, which may lead to damage, repair or both.[29] Charge transfer often arises in photosynthetic reaction centres, a complex of proteins and pigments, to conduct the primary energy conversion reaction in photosynthesis.[30] Recent fluorescence and Raman spectroscopic investigations of pH-dependent structure of DNA report that binding of protons to DNA bases leads to a conformational change.[25–28] Moreover, protons have been taken up by the protein in photosynthetic reaction centre upon electron transfer.[31] Therefore, study of acid concentration dependence of electron transfer processes in ICT molecules may supply preliminary yet critical information towards understanding of the charge transfer processes in complex biological systems. In such a scenario, the present study can be regarded as a model investigation involving relatively simpler (solvent + solute) systems, the results of which may stimulate suitable analytical works.

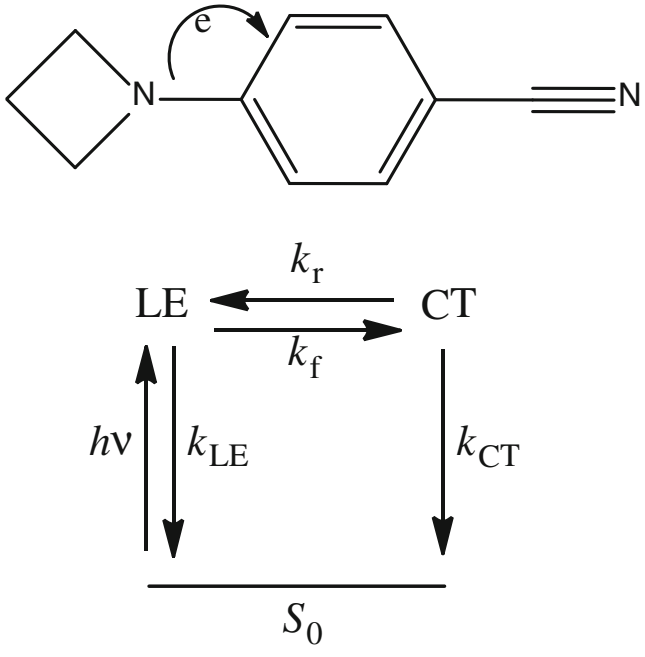

Scheme 1. Molecular structure of 4-(azetidinyl) benzonitrile (P4C) and various rate processes of the photo-induced charge transfer model (species in S_0 state can be P4C or its protonated form).

2. Measurement and computation details

2.1 *Spectroscopic measurements*

4-(Azetidinyl) benzonitrile (P4C) was synthesized using the method reported earlier.[32] Synthesized P4C was recrystallized twice from cyclohexane (Merck, Germany) and purity checked via thin-layer chromatography and excitation wavelength dependent fluorescence measurements in solvents of differing polarities. Acetonitrile (ACN), ethyl acetate (EA) and ethanol (EtOH) were obtained from Sigma-Aldrich and used as received. Hydrochloric acid (HCl) was purchased from Merck, India. Acid solutions with HCl at milli-molar concentrations have been prepared by mixing concentrated HCl (35%) in these solvents. Since these solvents (ACN, EA or EtOH) are sufficiently polar, dissociation of HCl will produce H^+ and Cl^- in them.

Steady state absorption, emission, and time-resolved fluorescence measurements were carried out following standard protocol described earlier.[17–20] Concentration of P4C in solutions was maintained always at $\leq 10^{-5}$M. Fluorescence spectra of P4C in polar solutions were deconvoluted into two segments (namely LE and CT) using a reference fluorescence spectrum of same solute in perfluorohexane.[16] Areas under the LE and CT bands so obtained were then used for further analyses. Fluorescence peak frequencies of LE and CT were calculated by adding the shifts of the peak frequency (with respect to reference spectra) in solutions with

reference frequency in perfluorohexane. Error associated with the peak frequency and width are typically ±150 cm^{-1} and ±200 cm^{-1}, respectively. Time resolved fluorescence intensity decays were measured using time-correlated single photon counting (TCSPC) technique (Lifespec-ps, Edinburgh). The full width at half maxima of the instrument response function (IRF) was ~450 ps when we used a 299 nm laser diode (PLS-8-2-232, PicoQuant) as excitation source having pulse width ~500 ps. In the present study and also in many previous studies,[16–20] the short time constants obtained from LE fluorescence decays were found to be very similar to the short time constants (rise-time) needed to fit the CT fluorescence decays of P4C. Therefore, the short time constant was considered as the reaction time of LE ↔ CT interconversion reaction.

2.2 *Computational study*

Geometry optimizations of P4C, protonated P4C, ethanol and protonated ethanol were performed for the ground state using density functional theory (DFT) method at B3LYP/6-31G(d) level of theory. No imaginary frequencies were available after vibration analysis of the optimized structures, which indicated that each of the optimized structures was at the real minimum on the potential energy surfaces (PES). Enthalpy changes for protonation were calculated by the energy differences between protonated and non-protonated species at optimized condition. Electronic transition energies and oscillator strengths were calculated using time-dependent density functional theory (TD-DFT) using the B3LYP functional and the 6-31G(d) basis set. All the above computations were carried out using the GAUSSIAN 09 program package.[33]

3. Results and discussion

3.1 *Steady state spectroscopic studies*

Figure 1 exhibits representative absorption and fluorescence spectra of the solute in ACN at three HCl concentrations in upper and lower panels, respectively. Note the blue shift in absorption spectrum upon increasing acid concentration. Fluorescence spectrum, as expected, shows both the normal band (due to locally excited, LE, state) and the red-shifted charge-transfer (CT) band.[16–18] Molecular structure and charge transfer process of P4C have been shown in scheme 1. It is evident that the area under the CT band decreases with increasing HCl concentration, which indicates that charge transfer is becoming unfavourable with acid

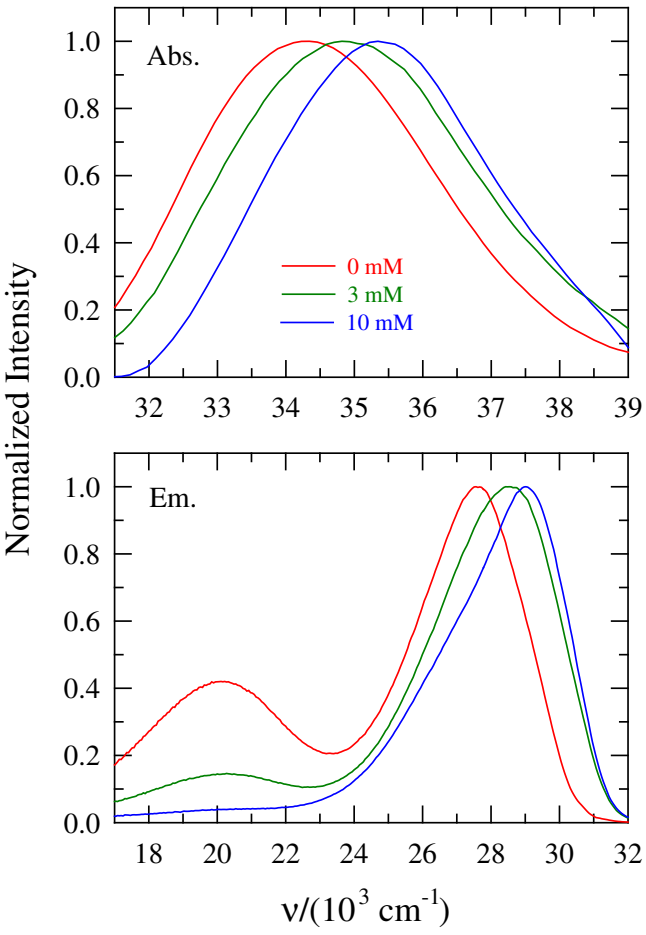

Figure 1. Representative absorption (upper panel) and emission (lower panel) spectra of P4C in ACN at various HCl concentrations.

concentration. Absorption and fluorescence intensities of P4C in all solvents also decrease with increasing HCl concentration with concomitant blue shift in both LE and CT peak positions. Absorption and emission spectra of P4C at few representative acid concentrations in EA and EtOH are shown in figures S1 and S2, respectively (Supplementary information). One point to note here that for a two-state model of protonation an isosbestic point is expected in absorption spectra. However, we did not find any isosbestic point in absorption spectra of P4C in all solvents. This may be due to the coexistence of more than two species.[34] As few, though extent is very less, doubly protonated species may be formed due to protonation at sp-hybridized N-atom of P4C.

The HCl concentration-dependent absorption and emission frequencies of P4C in all these solutions are presented in various panels of figure 2. Absorption spectrum of P4C shifts towards blue for all the solvents (ACN, EA and EtOH) while adding HCl into the solution. The observed shift is the largest for ACN and it

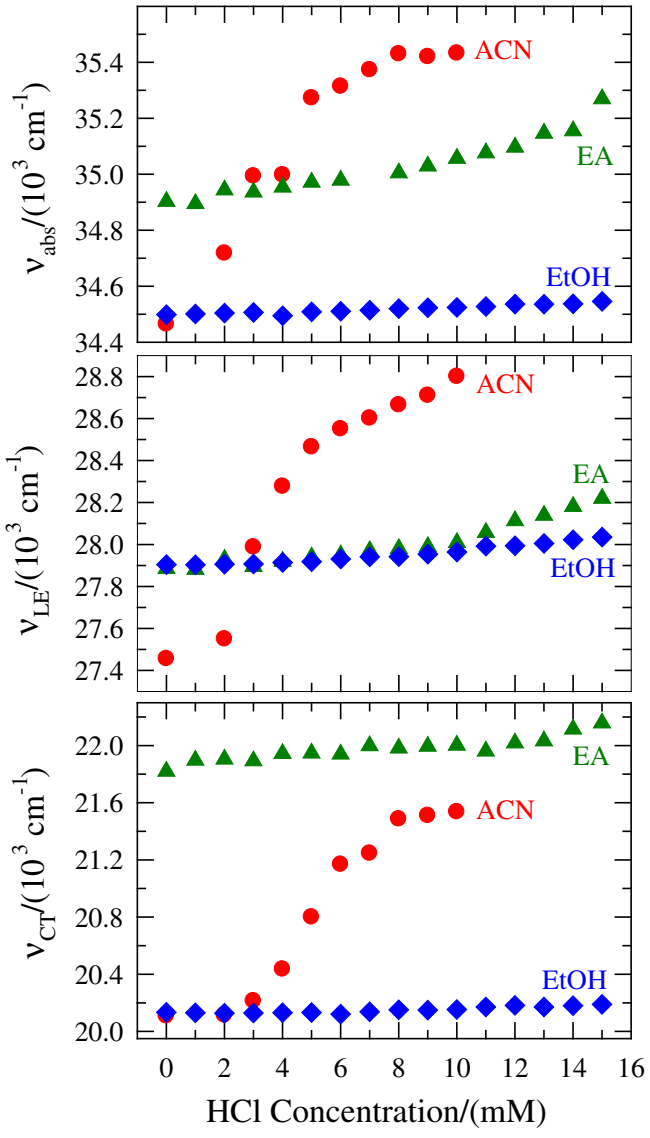

Figure 2. Acid concentration dependence of steady state absorption and emission spectral properties of P4C in solvents of differing polarities. While the upper panel represents absorption frequencies (ν_{abs}), the middle and lower panel, respectively, show LE (ν_{LE}) and CT (ν_{CT}) emission frequencies in ACN, EA and EtOH at various HCl concentrations (colour coded).

becomes ~1000 cm^{-1} at 10 mM HCl concentration. The spectral shift in EA is ~400 cm^{-1} at 15 mM HCl concentration. The least spectral shift occurs in EtOH, which is ~50 cm^{-1} at 15 mM concentration. The polarity order for the three solvents is as follows: EA ($\varepsilon_0 \approx 6$) < EtOH ($\varepsilon_0 \approx 24$) < ACN ($\varepsilon_0 \approx 36$).[16] Clearly, the effects of HCl on spectral shift do not follow the polarity order of these solvents. Another interesting aspect is that the blue shift is the maximum for solvents of the highest polarity considered here (ACN). The above phenomenon can be explained by considering the up-taking of proton by P4C molecule in acidic solutions.

Our TD-DFT calculations, described in the next section, suggests that absorption maximum of P4C may shift towards higher energy (that is, blue-shift) with addition of H^+. Earlier computational studies of proton-induced intramolecular charge transfer in donor-pi-acceptor molecule also showed a marked blue shift in absorption spectrum in presence of proton.[35] As ACN is a highly polar solvent, it can easily dissociate the added acid and supply proton for uptake by P4C. Moreover, in $E_T(30)$ scale of solvent polarity, ACN is relatively less polar ($E_T(30) \sim 45.6$ kcal mol^{-1}) compared to EtOH ($E_T(30) \sim 51.9$ kcal mol^{-1}), whereas EA possesses least polarity ($E_T(30) \sim 38.1$).[36] Eventhough both ACN and EtOH are sufficiently polar, EtOH can also accommodate a proton on its hydroxyl group or participate in H-bonding with HCl and thus become a competitor of P4C. This may weaken the effects of HCl on spectral shifts of P4C in EtOH. Another point to be mentioned here is that, among these solvents, dissociation constant of HCl is expected to be the largest in ACN because of its largest ε_0 among these three solvents. However, in the case of EtOH, a protonated alcohol possesses low pKa, which means dissociation constant of HCl would be the least.[37] Therefore, the insignificant change in spectral peak position with HCl concentration in EtOH may have originated from the relatively weaker dissociation of HCl in this solvent.

Similar to the absorption spectrum in ACN, the LE and CT frequencies also show a blue shift with increasing HCl concentration. While in ACN, the LE and CT fluorescence bands exhibit a blue shift of ~1300 cm^{-1}, a blue shift of ~350 cm^{-1} is observed in EA solutions. Insignificant change in LE and CT spectral frequencies with HCl concentration is seen for EtOH solutions. These facts could be explained by protonation of amine group and dissociation of HCl in different solvents. It is known that protonation of the amine group reduces the electron-donating properties of donor moiety and consequently charge transfer is hindered.[38] This is reflected in decrease of area under the CT band in ACN (see figure 1).

Figure 3 depicts the acid concentration dependence of the ratios between areas under the CT and LE fluorescence bands (α_{CT}/α_{LE}). An interesting feature in this figure is that the ratio, α_{CT}/α_{LE}, exhibits a significant decrease in ACN, it shows an increase in EtOH with acid concentration. In contrast, this remains insensitive to acid concentration in EA. As H^+ can occupy the electron density on nitrogen atom in P4C, the formation of CT state can be hindered in acid solutions. Consequently, α_{CT}/α_{LE} decreases with increasing acid concentration. However, as EtOH can take up protons in competition with P4C, the situation reverses as the ICT

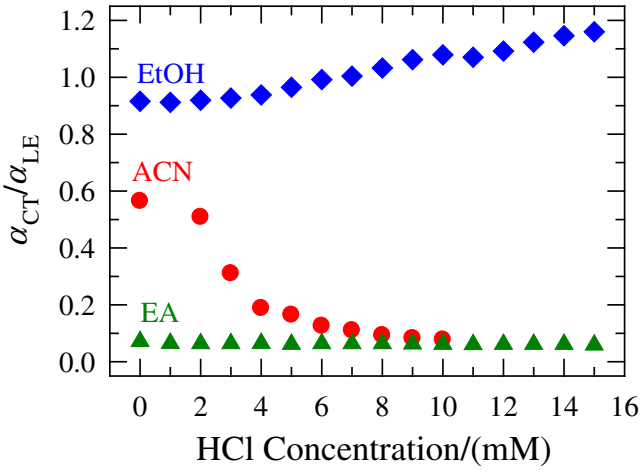

Figure 3. Acid concentration dependence of ratio (α_{CT}/α_{LE}) of areas under the CT and LE fluorescence bands of P4C in ACN, EA and EtOH (colour coded).

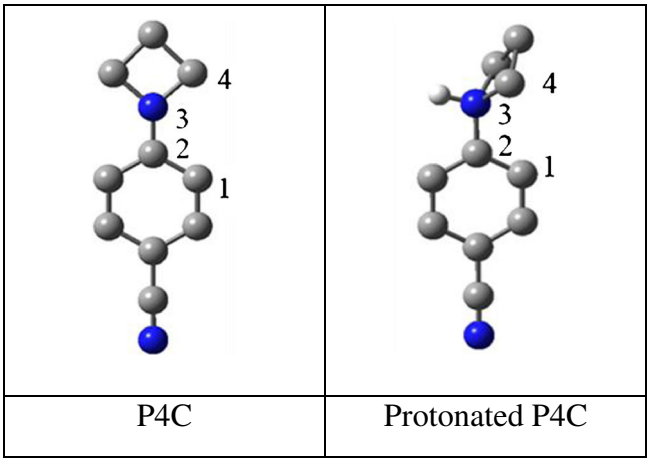

Figure 4. Optimized geometries of P4C and protonated P4C (conjugate acid), calculated at B3LYP/6-31G(d) level of theory. Grey, blue and white balls represent respectively, carbon, nitrogen and hydrogen atoms. Hydrogen atoms except in azetidinyl nitrogen are omitted for clarity.

process in P4C is not hindered as much as in other solvents. This may be the reason for α_{CT}/α_{LE} to increase by ∼25% at an acid concentration of 15 mM. The computational results presented below appear to support such a view.

3.2 *Computational studies*

Figure 4 shows the optimized structures of P4C and conjugate acid of P4C, which is formed after addition of H^+ with P4C. Dihedral angles (DHA) constituted with C1, C2, N3 and C4 in P4C and in its protonated form (conjugate acid, see figure 4), are respectively, 0.46 and −54.44°, which indicates that azetidinyl ring is nearly coplanar with benzene ring in P4C and this co-planarity is destroyed due to conjugate acid formation. Electron density is reduced due to conjugate acid formation which can be observed from the highest occupied molecular orbital (HOMO) surfaces in figure 5. Both these changes disfavour the charge transfer from azetidinyl ring to benzene moiety in conjugate acid of P4C, which may restrict the formation of charge transfer (CT) state. These are consistent with experimental results, where α_{CT}/α_{LE} decreases with acid concentration in acetonitrile and ethyl acetate. TD-DFT calculations show that absorption maxima of P4C in the gas phase may be shifted towards blue by ∼29 nm (264 nm → 235 nm) after adding H^+ provided we consider the electronic transition with highest oscillator strength (second singlet excited state S_2, table 1). The blue shift is also the same (∼29 nm) if we consider first singlet excited state (S_1). This supports the experimental large blue shift in absorption and emission spectra of P4C in presence of HCl. The protonation to the P4C also reduces the oscillator strength (table 1). Protonation to the P4C in ethanol competes with ethanol as it is a protic solvent. Enthalpy changes for the protonation of P4C and ethanol in gas phase, are respectively, −222.45 and −194.94 kcal/mol. Protonation for both cases is exothermic which indicates that protonation may occur spontaneously both in P4C and ethanol. However, protonation to P4C is thermodynamically more favourable than ethanol. Co-protonation of ethanol may be one reason for displaying reverse effect of HCl concentration on CT formation of P4C in ethanol (i.e., α_{CT}/α_{LE} increases with acid concentration) with respect to that in ethyl acetate and acetonitrile. In this case, average polarity dominates over acid effects for the CT formation in P4C.

3.3 *Time-resolved fluorescence emission studies*

Time resolved fluorescence spectra of P4C for LE state have been measured in all solvents at different acid concentrations. For a few cases, CT state decays have also been measured. The representative fluorescence transients of P4C for LE and CT states in ACN at 5 mM HCl are shown in figure 6 along with bi-exponential fits and residuals. Note the similarity between the short decay time constant for LE and the rise time for CT in these unconstrained fits. As discussed already, this time constant is identified here as the reaction time constant ($\langle\tau_{rxn}\rangle$). The other time resolved fluorescence decays have also been found to fit to bi-exponential functions

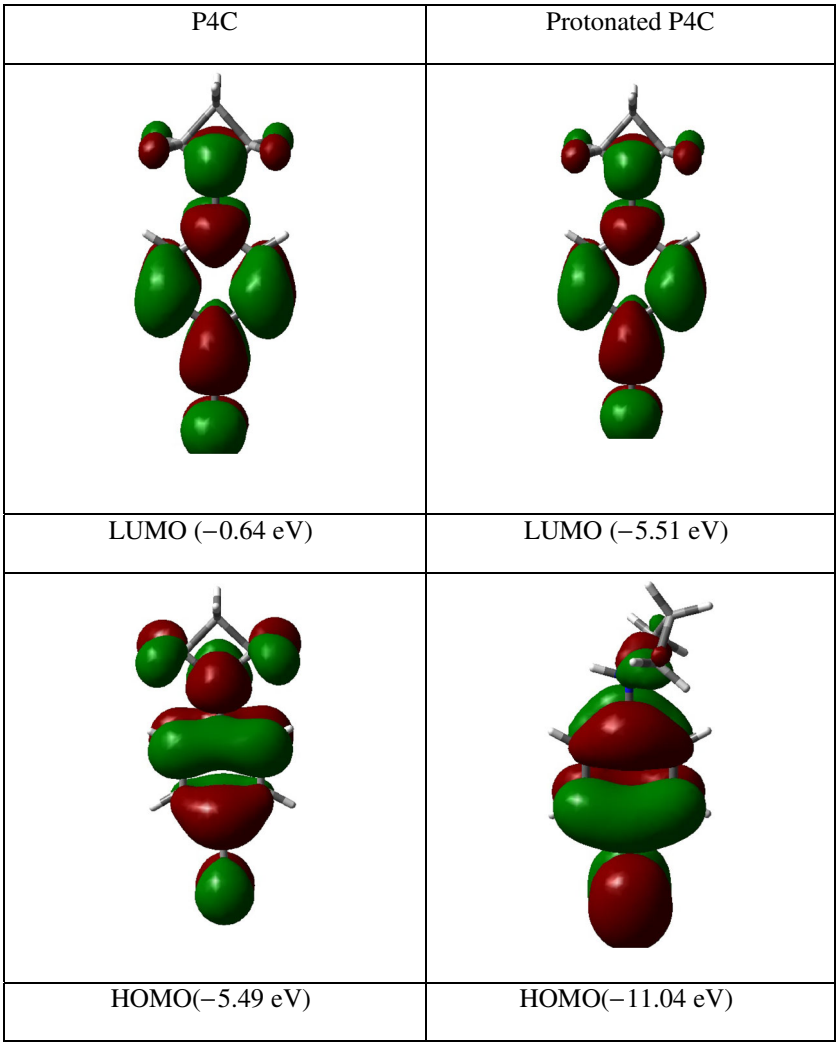

Figure 5. Frontier molecular orbital profiles of P4C and protonated P4C. Green and red correspond to the different phases of the molecular wave functions for the HOMOs (highest occupied molecular orbitals) and LUMOs (lowest unoccupied molecular orbitals), and the isovalue is 0.02 a.u. Orbital energies (eV) are given in parentheses.

of time. This suggests that ICT reaction in P4C in presence of acid in these polar solvents also conforms to the two-state description proposed earlier for a variety of medium.[16–20] Acid concentration dependence of $\langle\tau_{rxn}\rangle$ and LE fluorescence life time ($\langle\tau_{life}\rangle$, the long time constant associated with LE decays) are shown, respectively, in upper and lower panels of figure 7. It is interesting to note that $\langle\tau_{rxn}\rangle$ increases significantly (∼30%) upon addition of HCl in ACN and EA, but remains largely insensitive to acid concentration in EtOH. The

Table 1. Main excitations and oscillator strengths corresponding to first and second singlet excited state in P4C and protonated P4C: TDDFT calculations.

Comp.	Excited State	Excitations	Calc. λ (nm)	Oscillator strength
P4C	S_1	HOMO→LUMO+1 (66.99%)	274	0.025
	S_2	HOMO-1→LUMO+1 (12.40%) HOMO→LUMO (69.34%)	264	0.629
Protonated P4C	S_1	HOMO-1→LUMO (51.64%)	245	0.012
	S_2	HOMO-1→LUMO+1 (14.81%) HOMO→LUMO (67.11%)	235	0.354

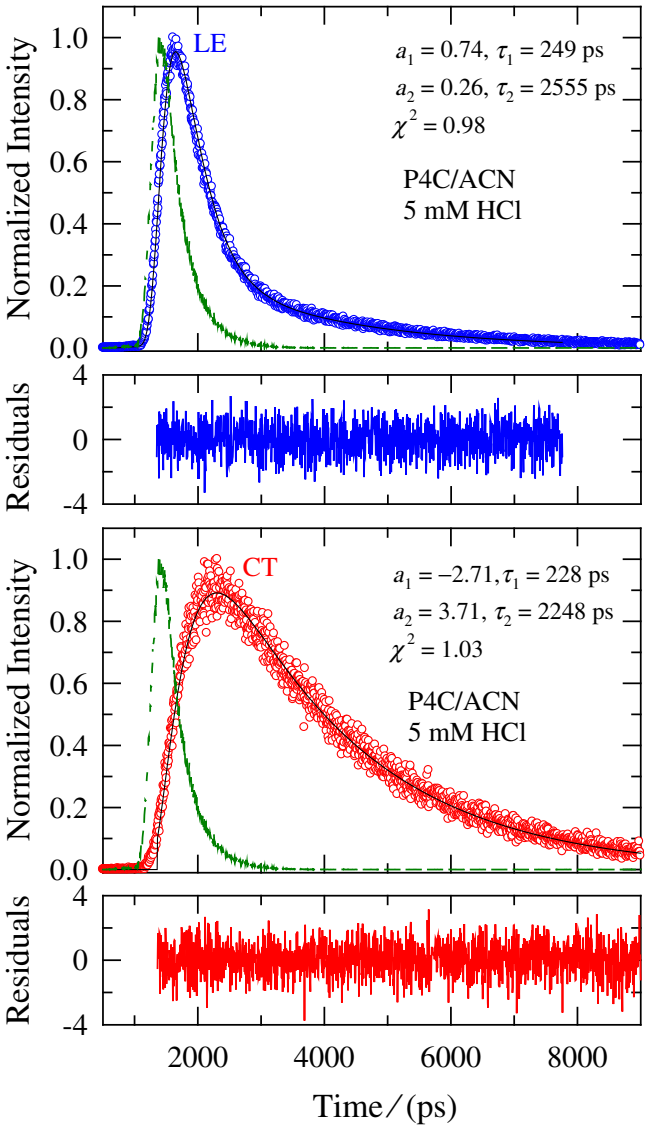

Figure 6. Representative normalized LE (upper panel) and CT (lower panel) emission decays of P4C in ACN at 5 mM HCl concentration. The data are represented by the circles, and the fit through the data are shown by solid lines. The instrument response function is shown by the broken line. The bi-exponential fit parameters are also provided in respective panels. The LE peak count was ∼3000 and the CT peak count was ∼1000.

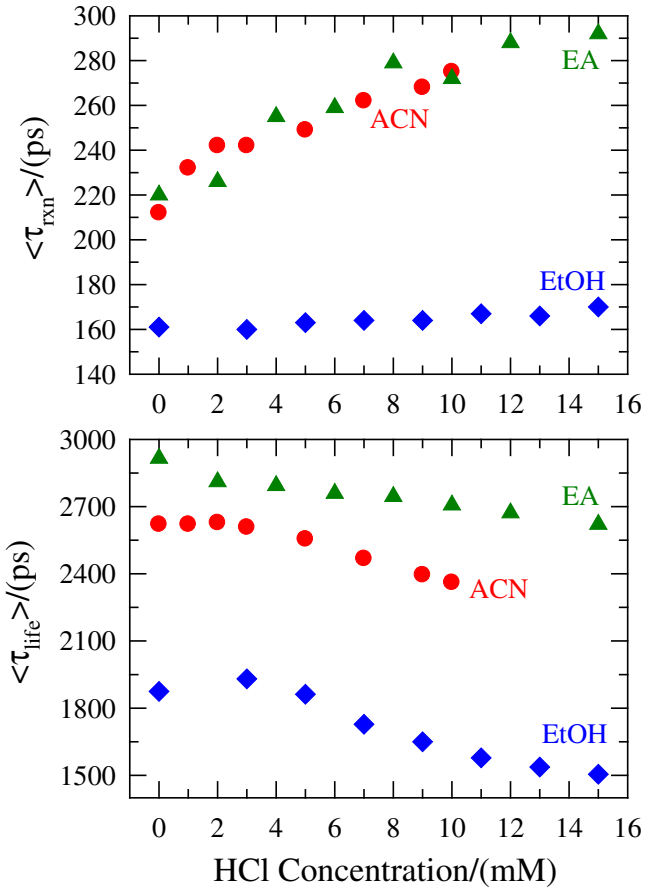

Figure 7. Acid concentration dependence of the fast (upper panel) and slow (lower panel) time constants of LE fluorescence decays associated with the LE → CT interconversion reaction of P4C in ACN, EA and EtOH (colour coded). The fast and slow time constants of the decays are the reaction time ($\langle\tau_{rxn}\rangle$) and life time ($\langle\tau_{life}\rangle$) of the solute in these solvents, respectively.

associated change in $\langle\tau_{life}\rangle$ is much less, being limited within ∼5–15% in these media.

One important point is, the state in which, ground or excited, P4C absorbs proton. Another point is how much does HCl dissociate in solution of these polar solvents, or, form H-bond partially with azetidinyl nitrogen in P4C. If P4C molecule absorbs proton in the ground state, then for this molecule, possibility of participating in charge transfer reaction in the excited state reduces. On the other hand, if the molecule makes H-bond with HCl in the ground state, the molecule can still participate in the charge transfer reaction but with reduced affinity. Similar phenomenon may occur if the molecule absorbs proton or makes H-bond in the excited state also. DFT, calculations show that twist angle (dihedral angle between the two planes containing azetidine and benzonitrile moieties) may change by 55° if the molecule absorbs proton in the gas phase. Reduced electron density in the excited state and restricted rotation of donor moiety (azetidinyl) can jointly reduce the reaction rate in ACN or EA in presence of acid. Insensitivity of $\langle\tau_{rxn}\rangle$ to HCl concentration in EtOH also supports the minimal variation of steady state absorption and fluorescence spectral features. Least dissociation of HCl in EtOH[37] does not alter the rate of charge transfer reaction appreciably. Eventhough, $\langle\tau_{rxn}\rangle$ does not exhibit any dependence, the relative amplitude associated with it has been seen to decrease (∼15%) with HCl concentration in EtOH. However, in ACN and EA, relative amplitudes do not

show any dependence on acid concentration (shown in table S1 of Supplementary information). Dependence of $\langle\tau_{life}\rangle$ on acid concentration may arise due to additional non-radiative decay channels provided by H-bonding and/or protons from the added acid.

4. Conclusion

Dependence on acid concentration of LE ↔ CT interconversion reaction in aprotic (ACN, EA) and protic (EtOH) solvents has been explored. Steady state spectroscopic studies revealed that HCl concentration effects are stronger in ACN than in EA. The absorption and emission (LE and CT) band frequencies shifted towards blue with HCl concentration in ACN and EA, whereas no significant dependence has been observed in ethanolic solutions. These blue shifts are believed to arise from the protonation of the donor moiety of P4C, suggesting the extent of protonation in ACN and EA is stronger than in EtOH. CT/LE area ratio increases markedly with acid concentration in ACN, but decreases in EtOH. This suggests that solvent association character can determine the effects of added acid on intramolecular reaction. The reaction rate constant shows significant dependence on HCl concentration in ACN and EA; no or insignificant dependence has been found in EtOH. This fact also supports that the extent of protonation of azetidinyl nitrogen is greater in ACN and EA and weaker in EtOH. Therefore, results obtained from steady state as well as time-resolved measurements support the same inference. TDDFT calculations provide further support for the observed acid-induced blue-shift in ACN and EA, but not in EtOH. The study presented here needs further sophisticated experimental studies and theoretical investigation for quantitative explanation of acid concentration dependence of charge transfer reaction.

Supplementary information

Absorption and emission spectra of P4C in EA and EtOH, and biexponential fit parameters of fluorescence intensity decays associated with LE band of P4C in ACN, EA and EtOH at various HCl concentrations are provided as Supplementary information (figures S1–S2 and table S1) can be seen in www.ias.ac.in/chemsci.

Acknowledgements

We thank anonymous reviewers for insightful comments which immensely helped improving the quality of the manuscript. BG thanks Council of the Scientific and Industrial Research (CSIR), New Delhi, India and SN Bose National Centre for Basic Sciences, Kolkata for providing fellowship.

References

1. Jortner J and Bixon M (eds) 1999 *Adv. Chem. Phys.* **106** 107
2. Bach U, Luppo D, Comte P, Moser J E, Weissörtel F, Salbeck J, Spreitzer H and Grätzel M 1998 *Nature* **395** 583
3. Clayton R K 1980 *Photosynthesis: Physical mechanisms and chemical patterns* (Cambridge: Cambridge University Press)
4. Siders P, Cave R J and Marcus R A 1984 *J. Chem. Phys.* **81** 5613
5. Chandra A and Bagchi B 1991 *J. Chem. Phys.* **94** 8367
6. Eads D D, Dismer B G and Fleming G R 1990 *J. Chem. Phys.* **93** 1136
7. Pradhan T, Ghoshal P and Biswas R 2008 *J. Phys. Chem. A* **112** 915
8. Grabowski Z R, Rotkiewicz K and Rettig W 2003 *Chem. Rev.* **103** 3899
9. Lai R Y, Fabrizio E F, Lu L, Jenekhe S A and Bard A J 2001 *J. Am. Chem. Soc.* **123** 9112
10. He C, He Q, He Y, Li Y, Bai F, Yang C, Ding Y, Wang L and Ye J Sol 2006 *Energy Mater. Sol. Cells* **90** 1815
11. (a) Santhosh K and Samanta A 2010 *J. Phys. Chem. B* **114** 9195; (b) Li X, Liang M, Chakraborty A, Kondo M and Maroncelli M 2011 *J. Phys. Chem. B* **115** 6592
12. Datta A, Mandal D, Pal S K and Bhattacharyya K 1997 *J. Phys. Chem.* **B101** 10221
13. Biswas R, Rohman N, Pradhan T and Buchner R 2008 *J. Phys. Chem. B* **112** 9379
14. Pradhan T, Gazi H, Guchhait B and Biswas R 2012 *J. Chem. Sci.* **124** 355
15. Wan C, Fiebig T, Schiemann O, Barton J K and Zewail A H 2000 *Proc. Natl. Acad. Sci. USA* **97** 14052
16. (a) Dahl K, Biswas R, Ito N and Maroncelli M 2005 *J. Phys. Chem. B* **109** 1563; (b) Techert S and Zachariasse K A 2004 *J. Am. Chem. Soc.* **126** 5593
17. Pradhan T and Biswas R 2007 *J. Phys. Chem. A* **111** 11514
18. Pradhan T and Biswas R 2009 *J. Sol. Chem.* **38** 517
19. Pradhan T, Gazi H A R and Biswas R 2009 *J. Chem. Phys.* **131** 054507
20. Gazi H A R and Biswas R 2011 *J. Phys. Chem. A* **115** 2447
21. (a) Wang D and Imae T 2004 *J. Am. Chem. Soc.* **126** 13204; (b) Baruah M, Qin W, Flors C, Hofkens J, Vallée R A L, Beljonne D, Van der Auweraer M, De Borggraeve W M and Boens N 2006 *J. Phys. Chem. A* **110** 5998
22. Violot S, Carpentier P, Blanchoin L and Bourgeois D 2009 *J. Am. Chem. Soc.* **131** 10356
23. Moreno-Villoslada I, Jofré M, Miranda V, González R, Sotelo T, Hess S and Rivas B L 2006 *J. Phys. Chem. B* **110** 11809
24. Klegeris A, Korkina L G and Greenfield S A 1995 *Free Radical Biol. Med.* **18** 215

25. Hsu S T, Blaser G, Behrens C, Cabrita L D, Dobson C M and Jackson S E 2010 *J. Biol. Chem.* **285** 4859
26. Pots A M, de Jongh H H J, Gruppen H, Hessing M and Voragen A G 1998 *J. Agric. Food Chem.* **46** 2546
27. Choi J, Kim S, Tachikawa T, Fujitsuka M and Majima T 2011 *J. Am. Chem. Soc.* **133** 16146
28. O'Connor T, Mansy S, Bina M, McMillin D R, Bruck M A and Tobias R S 1982 *Biophys. Chem.* **15** 53
29. Dandliker P J, Núñez M E and Barton J K 1998 *Biochemistry* **37** 6491
30. Fleming G R, Martin J L and Breton J 1988 *Nature* **333** 190
31. Miksovska J, Schiffer M, Hanson D K and Sebban P 1999 *Proc. Natl. Acad. Sci. USA* **96** 14348
32. Rettig W 1981 *J. Lumin.* **26** 21
33. Frisch M J, Trucks G W, Schlegel H B, Scuseria G E, Robb M A, Cheeseman J R, Scalmani G, Barone V, Mennucci B, Petersson G A, Nakatsuji H, Caricato M, Li X, Hratchian H P, Izmaylov A F, Bloino J, Zheng G, Sonnenberg J L, Hada M, Ehara M, Toyota K, Fukuda R, Hasegawa J, Ishida M, Nakajima T, Honda Y, Kitao O, Nakai H, Vreven T, Montgomery J A, Peralta J E, Ogliaro F, Bearpark M, Heyd J J, Brothers E, Kudin K N, Staroverov V N, Keith T, Kobayashi R, Normand J, Raghavachari K, Rendell A, Burant J C, Iyengar S S, Tomasi J, Cossi M, Rega N, Millam J M, Klene M, Knox J E, Cross J B, Bakken V, Adamo C, Jaramillo J, Gomperts R, Stratmann R E, Yazyev O, Austin A J, Cammi R, Pomelli C, Ochterski J W, Martin R L, Morokuma K, Zakrzewski V G, Voth G A, Salvador P, Dannenberg J J, Dapprich S, Daniels A D, Farkas O, Foresman J B, Ortiz J V, Cioslowski J, Fox D J 2010 *Gaussian 09,* Revision B. 01 Gaussian Inc.: Wallingford CT
34. Vinokurov I A and Kankare J 1998 *J. Phys. Chem. B* **102** 1136
35. Liu X, Wang N, Lv L and Cai L 2011 *Comput. Theor. Chem.* **978** 29
36. Reichardt C 1994 *Chem. Rev.* **94** 2319
37. Bruice P Y 2006 *Essential organic chemistry* (2nd ed.), Pearson Education (United States)
38. Zhao G-J, Chen R-K, Sun M-T, Liu J-Y, Li G-Y, Gao Y-L, Han K-L, Yang X-C and Sun L 2008 *Chem. Eur. J.* **14** 6935